

INFLUENCE OF THE SHEAR STRESS σ_4 ON THE PHYSICAL PROPERTIES OF ROCHELLE SALT

R. R. Levitskii¹, I. R. Zachek², A. P. Moina¹, T. M. Verkholyak¹

¹*Institute for Condensed Matter Physics of the National Acad. Sci. of Ukraine,
1 Svientsitskii Str., Lviv, UA-79011, Ukraine*

²*State University "Lvivs'ka Politehnika",
12 Bandera Str., Lviv, UA-79013, Ukraine*

(Received March 19, 2002; received in final form August 14, 2002)

We study the influence of shear stress σ_4 on the phase transitions, static and dynamic dielectric, piezoelectric, elastic, and thermal characteristics of Rochelle salt crystal. The stress effects are visible in the ferroelectric phase and in some temperature range below T_{C1} and above T_{C2} . The stress smears out the two second order phase transitions in Rochelle salt and smoothens the peculiarities in temperature curves of the second derivatives of thermodynamic potential χ_{11}^σ , χ_{11}^ϵ , d_{14} , e_{14} , c_{44}^E and s_{44}^E , as well as ϵ_{11}^* . Stress effects on these quantities are more essential near the upper Curie point. The characteristics that only exhibit bends at the transition points (c_{44}^P , h_{14} , g_{14}) are not affected by σ_4 . Stress dependence of the magnitude of the specific heat peaks at the 'transition points' is not monotonic and more pronounced near the lower 'Curie point'.

Key words: Rochelle salt, shear stress, piezoelectricity.

PACS number(s): 77.22.Ch, 77.22.Gm, 77.65.Bn, 77.65.Ly, 77.80.Bh

I. INTRODUCTION

It is generally accepted that Rochelle salt undergoes two ferroelectric phase transitions. The ferroelectric phase exists in a rather narrow temperature interval from $T_{C1} = 255$ K to $T_{C2} = 297$ K. Spontaneous polarization is directed along the a axis; it is accompanied by a spontaneous shear strain ϵ_4 in the plane (100). In both the low-temperature ($T < T_{C1}$) and high-temperature ($T > T_{C2}$) phases the crystal lattice belongs to the rhombic space group, whereas in the ferroelectric phase the crystal is monoclinic.

Microscopic theories of Rochelle salt type crystals are usually based on the Mitsui model [1]. Thermodynamics and dielectric properties of Rochelle salt within this model have been extensively studied by Vaks [2], Zeks *et al* [3,4], Mori [5], Kalenik [6], Levitskii *et al* [7,8]. Within the model that does not take into account the piezoelectric coupling, however, incorrect temperature dependence of relaxation times (diverging) and dynamic permittivity (vanishing) were obtained near the Curie points. The problem has been successfully approached in our recent paper by explicit taking into account the piezoelectric effects [9]. It permitted to distinguish between the free and clamped permittivities and obtain finite relaxation times at the Curie points.

Essential to the understanding of such crucial phenomena in ferroelectrics as processes of repolarization, domain wall motion, etc. are studies of these processes in external fields conjugate to spontaneous polarization. For piezoelectric ferroelectrics such fields are an electric field applied along the axis of spontaneous polarization as well as mechanical stress producing lattice strain conjugate to polarization. For Rochelle salt those fields are:

the electric field E_1 and the shear stress σ_4 . In the above studies of the domain processes sometimes it is necessary to know the stress/field dependences of the physical characteristics of a single-domain crystal. To calculate such dependences of static and dynamic dielectric, piezoelectric, elastic, and thermal properties of Rochelle salt is the purpose of the present paper.

A general idea of the field effects on the system undergoing a second order phase transition is well-known. Such a field is expected to smear out the phase transition, induce non-zero polarization in the paraelectric phase, as well as round off and decrease the peak values of the dielectric permittivity. The situation with Rochelle salt, however, is more complicated, for it undergoes two phase transitions, and the 'paraelectric' phases are, in fact, antiferroelectric ones. It is interesting to compare the stress effects on the two Curie points, and to explore its influence on the other characteristics, such as specific heat.

Within a Mitsui model, modified by taking into account the shear strain ϵ_4 [9], we have recently calculated several dielectric, piezoelectric, thermal, and elastic characteristics of Rochelle salt and obtained a fair description of experimental data. In this paper we present only the final results for the above mentioned characteristics and study their dependences on stress σ_4 .

II. DIELECTRIC, ELASTIC, PIEZOELECTRIC, AND THERMAL CHARACTERISTICS OF ROCHELLE SALT

According to the Mitsui model, the phase transitions in Rochelle salt are caused by motion of dipoles in asym-

metric double-well potentials with two different interaction constants for the dipoles of the same and of different sublattices. The system Hamiltonian reads [9]

$$\begin{aligned} \hat{H} = & \frac{N}{2} v c_{44}^{0E} \varepsilon_4^2 - N v e_{14}^0 \varepsilon_4 E_1 - \frac{N}{2} v \chi_{11}^{\varepsilon_0} E_1^2 \\ & - \frac{1}{2} \sum_{qq'} \sum_{ff'=1}^2 R_{qq'}(ff') \frac{\sigma_{qf}}{2} \frac{\sigma_{q'f'}}{2} \\ & - \Delta \sum_q \left(\frac{\sigma_{q1}}{2} - \frac{\sigma_{q2}}{2} \right) - (\mu_1 E_1 - 2\psi_4 \varepsilon_4) \sum_q \sum_{f=1}^2 \frac{\sigma_{qf}}{2}. \end{aligned} \quad (2.1)$$

The three first terms in (2.1) represent the elastic, piezoelectric, and electric energies that do not depend on orientation of quasispins; $v = \bar{v} k_B$ is the unit cell volume. The quantity Δ describes an asymmetry of the double-well potential; μ_1 is the effective dipole moment. The last term in the Hamiltonian is an additional internal field produced by piezoelectric coupling with the shear strain ε_4 ; ψ_4 is the so-called deformational potential.

Hereafter we restrict ourselves by the mean field approximation. After straightforward calculations we obtain the thermodynamic potential of the considered system

$$\begin{aligned} \frac{g_{1E}}{N k_B} = & \frac{1}{2} \bar{v} c_{44}^{0E} \varepsilon_4^2 - \bar{v} e_{14}^0 \varepsilon_4 E_1 - \frac{1}{2} \bar{v} \chi_{11}^{\varepsilon_0} E_1^2 + \\ & + \frac{1}{4} (\tilde{J} + \tilde{K}) \xi^2 + \frac{1}{4} (\tilde{J} - \tilde{K}) \sigma^2 - 2T \ln 2 - \\ & - T \ln \cosh \frac{1}{2} (\gamma + \delta) - T \ln \cosh \frac{1}{2} (\gamma - \delta) - \bar{v} \sigma_4 \varepsilon_4. \end{aligned} \quad (2.2)$$

Here $\tilde{J} = J/k_B$ and $\tilde{K} = K/k_B$ are normalized per Boltzmann constant Fourier transforms at $\mathbf{q} = \mathbf{0}$ of potentials of interaction between quasispins belonging to the same and to different sublattices, respectively; σ_4 is shear stress conjugate to the strain ε_4 , whereas ξ and σ are the ferroelectric and antiferroelectric ordering parameters, defined via the single-particle distribution functions $\eta_f = \eta_{qf} = \langle \sigma_{qf} \rangle$

$$\xi = \frac{1}{2} (\eta_1 + \eta_2), \quad \sigma = \frac{1}{2} (\eta_1 - \eta_2),$$

and obeying the system of equations

$$\xi = \frac{\sinh \gamma}{\cosh \gamma + \cosh \delta}, \quad \sigma = \frac{\sinh \delta}{\cosh \gamma + \cosh \delta}, \quad (2.3)$$

where

$$\begin{aligned} \gamma = & \beta \left(\frac{J+K}{2} \xi - 2\psi_4 \varepsilon_4 + \mu_1 E_1 \right), \\ \delta = & \beta \left(\frac{J-K}{2} \sigma + \Delta \right). \end{aligned}$$

Thermodynamic equilibrium conditions yield equations for the strain ε_4 and polarization P_1

$$\sigma_4 = c_{44}^{0E} \varepsilon_4 - e_{14}^0 E_1 + 2 \frac{\psi_4}{\bar{v}} \xi, \quad (2.4)$$

$$P_1 = e_{14}^0 \varepsilon_4 + \chi_{11}^{\varepsilon_0} E_1 + \frac{\mu_1}{v} \xi. \quad (2.5)$$

Second derivatives of the thermodynamic potential are: the coefficient of piezoelectric stress

$$\epsilon_{14} = \left(\frac{\partial P_1}{\partial \varepsilon_4} \right)_{E_1} = e_{14}^0 - \beta \psi_4 \frac{\mu_1}{v} f(\xi, \sigma), \quad (2.6)$$

clamped static dielectric susceptibility

$$\chi_{11}^{\varepsilon} (0, T, \sigma_4) = \left(\frac{\partial P_1}{\partial E_1} \right)_{\varepsilon_4} = \chi_{11}^{\varepsilon_0} + \beta \bar{v} \frac{\mu_1^2}{2v^2} f(\xi, \sigma), \quad (2.7)$$

and the elastic constant at constant field

$$c_{44}^E = \left(\frac{\partial \sigma_4}{\partial \varepsilon_4} \right)_{E_1} = c_{44}^{0E} - \frac{2\beta \psi_4^2}{v} f(\xi, \sigma), \quad (2.8)$$

where

$$f(\xi, \sigma) = \frac{1}{\Delta_4} \left[\varkappa_4 (\cosh \gamma + \cosh \delta) - \beta (J - K) (\varkappa_4^2 - \xi \sigma \sinh \delta \sinh \gamma) \right],$$

$$\Delta_4 = (\cosh \gamma + \cosh \delta)^2 - \beta J \varkappa_4 (\cosh \gamma + \cosh \delta) - \left(\frac{\beta}{2} \right)^2 (J^2 - K^2) (\varkappa_4^2 - \xi \sigma \sinh \delta \sinh \gamma),$$

$$\varkappa_4 = \cosh \gamma - \xi \sinh \gamma = \cosh \delta - \sigma \sinh \delta = \frac{1 + \cosh \gamma \cosh \delta}{\cosh \gamma + \cosh \delta}.$$

The rest of piezoelectric, elastic, and dielectric characteristics can be expressed via the found above.

To calculate specific heat we use the entropy

$$\frac{S}{R} = 2 \ln 2 + \ln \cosh \frac{1}{2}(\gamma + \delta) + \ln \cosh \frac{1}{2}(\gamma - \delta) - \gamma\xi - \delta\sigma,$$

R is the gas constant. Molar specific heat of a quasispin subsystem at constant stress then reads

$$\Delta C_4^{\sigma_4} = -T \left(\frac{dS}{dT} \right)_{\sigma} = q_4^{P_1, \varepsilon_4} + q_{\xi}^{\varepsilon_4} p_{\xi}^{\sigma_4} + q_{\sigma}^{\varepsilon_4} p_{\sigma}^{\sigma_4} + q_4^p \alpha_4, \quad (2.9)$$

where

$$q_4^{P_1, \varepsilon_4} = T \left(\frac{\partial S}{\partial T} \right)_{P_1, \varepsilon_4} = R \left[(\gamma^2 + \delta^2) \frac{\rho}{2} - 2\gamma\delta\xi\sigma \right],$$

$$q_{\xi}^{\varepsilon_4} = T \left(\frac{\partial S}{\partial \xi} \right)_{\varepsilon_4, T} = \frac{v}{\mu_1} R \frac{\tilde{J} + \tilde{K}}{4} [-\gamma\rho + 2\delta\xi\sigma],$$

$$q_{\sigma}^{\varepsilon_4} = T \left(\frac{\partial S}{\partial \sigma} \right)_{\varepsilon_4, T} = \frac{v}{\mu_1} R \frac{\tilde{J} - \tilde{K}}{4} [-\delta\rho + 2\gamma\xi\sigma],$$

$$q_4^{P_1} = T \left(\frac{\partial S}{\partial \varepsilon_4} \right)_{P_1, T} = R \tilde{\psi}_4 [\gamma\rho - 2\delta\xi\sigma],$$

$\tilde{\psi}_4 = \psi_4/k_B$; α_4 is the coefficient of thermal expansion

$$\alpha_4 = \left(\frac{\partial \varepsilon_4}{\partial T} \right)_{\sigma_4} = \frac{-p_4 + h_{14} p_{\xi}^{\varepsilon_4}}{c_{44}^{\sigma_4}}. \quad (2.10)$$

Rather cumbersome expressions for $p_{\xi}^{\sigma_4}$ and $p_{\sigma}^{\sigma_4}$ are given in Appendix.

Dynamic properties of the system with Hamiltonian (2.1) are studied within the Glauber method [10]. In this approach, assuming that the strain is time independent (due to clamping of the crystal above the frequency of piezoelectric resonance), at small deviations of the system from equilibrium, we obtain the complex dielectric permittivity with two relaxation times

$$\varepsilon_{11}^*(\omega) = \varepsilon_{\infty} + \frac{4\pi\chi_1}{1 - i\omega\tau_1} + \frac{4\pi\chi_2}{1 - i\omega\tau_2}, \quad (2.11)$$

where

$$\chi_{1,2} = \frac{\mu^2}{v k_B} \frac{1}{2T} \frac{\tau_1 \tau_2}{\tau_2 - \tau_1} (\pm K^{(1)} \mp \tau_1 K^{(0)}), \quad (2.12)$$

and τ_f are relaxation times

$$\tau_{1,2}^{-1} = \frac{1}{2} \left\{ K_1 \mp \sqrt{K_1^2 - 4K_0} \right\}. \quad (2.13)$$

The used the notations are also presented in Appendix.

III. DISCUSSION

The fitting procedure has been in details described elsewhere. The found model parameters, providing a fair description of the presented above physical characteristics of Rochelle salt, are:

$$\tilde{J} = 797.36 \text{ K}, \quad \tilde{K} = 1468.83 \text{ K}, \quad \tilde{\Delta} = 737.33 \text{ K}, \\ \tilde{\psi}_4 = -760 \text{ K}, \quad c_{44}^{E_0} = 12.8 \cdot 10^{10} \text{ dyn/cm}^2, \quad \alpha = 1.7 \cdot 10^{-13} \text{ c}^{-1}.$$

The effective dipole moment μ_1 is taken as a decreasing function of temperature

$$\mu_1 = [2.52 + 0.0066(297 - T)] \cdot 10^{-18} \text{ esu} \cdot \text{cm}.$$

The temperature dependence of the crystal volume per two quasispins (half of the unit cell volume) is obtained from structural experimental data of [11]

$$v = 0.5219 \cdot [1 + 0.00013(T - 190)] \cdot 10^{-21} \text{ cm}^3.$$

Let us explore now the influence of shear stress σ_4 on the dielectric, piezoelectric, elastic, and thermal characteristics of Rochelle salt.

The stress σ_4 in this case is a field conjugate to the order parameter. Since both phase transitions are of the second order, the stress σ_4 smears them out. It induces non-zero values of polarization P_1 (and strain ε_4) in paraelectric phases and increases these quantities in the ferroelectric phase (Fig. 1). The obtained stress effects of the strain ε_4 are similar to those of polarization and more pronounced.

Theoretical dependence of spontaneous polarization P_1 on stress σ_4 qualitatively agrees with the old results of measurements presented in [12]. However, a quantitative comparison of the theoretical curves with the experimental points is not possible, because in [12] the polarization curves are given in arbitrary units different for different stresses.

In Fig. 2 we plot the temperature curves of a free static dielectric susceptibility at different values of stress σ_4 , as well as on the stress σ_4 at different temperatures. The corresponding dependences of the other characteristics — second derivatives of the thermodynamic potential, which have sharp peaks at the transition points — clamped dielectric susceptibility, coefficients of piezoelectric strain and piezoelectric stress, as well as elastic compliance $s_{44}^E = 1/c_{44}^E$, are analogous.

On increasing σ_4 , the magnitudes of χ_{11}^{σ} , χ_{11}^{ε} , d_{14} , e_{14} , and s_{44}^E decrease, especially fast at temperatures close to T_{Cf} and at small stresses (at ambient pressure χ_{11}^{σ} , d_{14} , and s_{44}^E diverge at the Curie points). The peak values of these quantities at the lower ‘transition point’ are essentially decreased and shifted to lower temperatures, whereas those at the upper ‘transition point’ are shifted to upper temperatures. A decrease of the peak values at

the upper ‘transition point’ is stronger than at the lower one. As calculations show, the presented characteristics depend on the stress only in a certain temperature range — starting from temperature somewhat lower than the lower transition point up to the temperatures somewhat higher than the upper transition point, including the ferroelectric phase (at the presented stresses — from 235 K up to 330 K). The temperature range of visible stress effects above T_{C2} is wider than below T_{C1} .

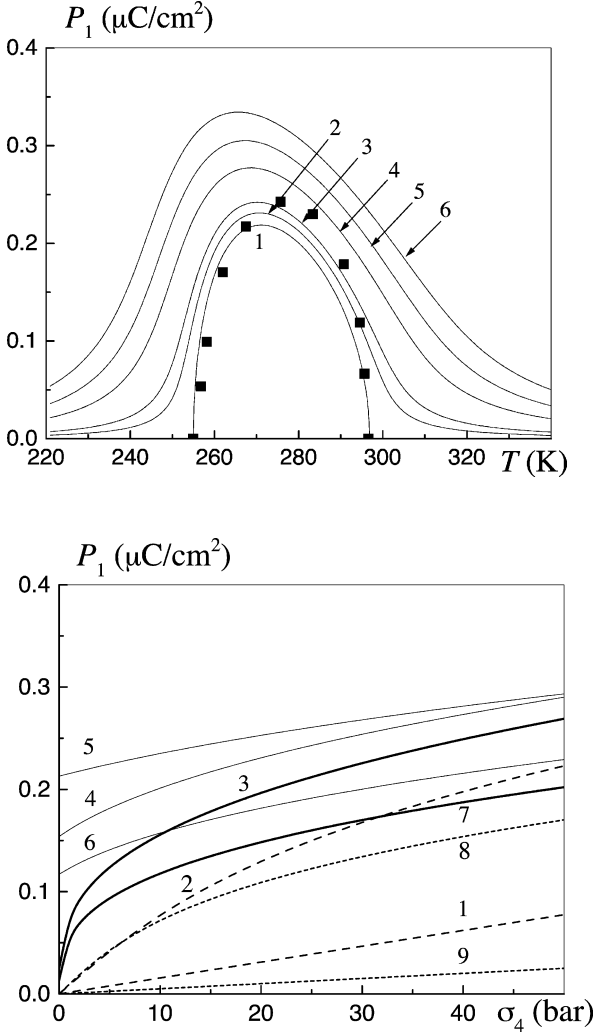


Fig. 1. Dependences of polarization P_1 on temperature at different stresses σ_4 (bar): 1 — 0, 2 — 5, 3 — 10, 4 — 30, 5 — 50, 6 — 75 and on stress σ_4 at different temperatures (K): 1 — 235 (dashed line), 2 — 250 (dashed line), 3 — 255.1 (thick solid line), 4 — 259, 5 — 276, 6 — 292 (thick solid lines), 7 — 296.8 (thick solid line), 8 — 302, 9 — 350 (dotted lines). Experimental points are taken from [13].

As an analog of the stress dependence of the first order transition temperature, in the case of the second order phase transition we plot the dependences for the temperatures of the rounded maxima of the dielectric susceptibility (‘transition temperature’ or ‘Curie point’).

As one can see (fig. 3), the upper ‘transition temper-

ature’ in Rochelle salt is stronger affected by stress σ_4 than the lower one, and stress dependences of the both ‘transition temperatures’ are essentially non-linear. This drastically differs from the almost linear dependence of the temperature of the first order phase transition in, for instance, KD_2PO_4 on the stress σ_6 [15].

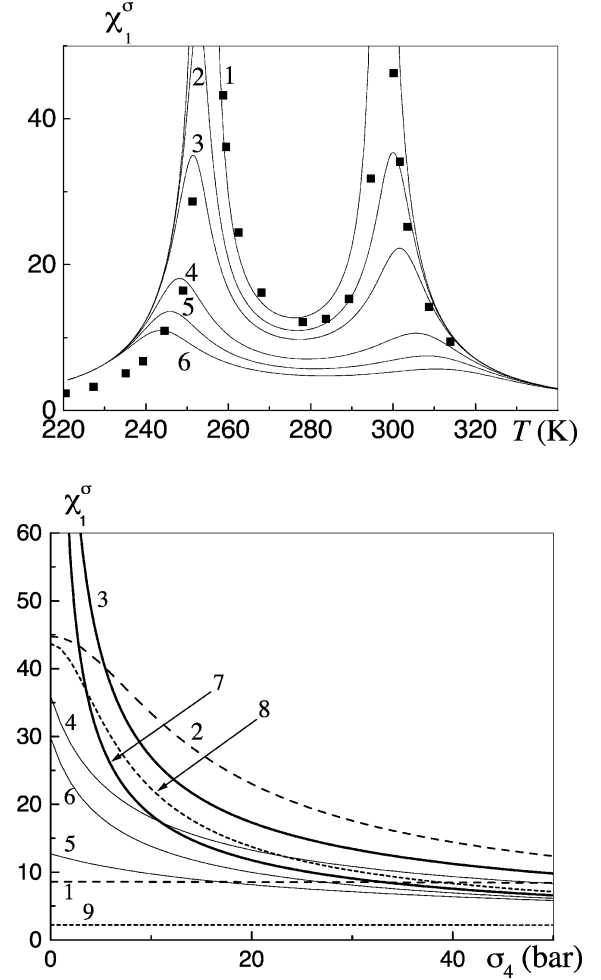


Fig. 2. Dependences of a free dielectric susceptibility χ_{11}^σ on temperature at different stresses σ_4 and on stress σ_4 at different temperatures. Notations, values of temperature and stress are the same as in Fig. 1. Experimental points are taken from [14].

The Landau theory (expansion up to P^4) predicts that dependences of the susceptibility peak magnitude χ_{\max} and its temperature ΔT_{\max} on external field conjugate to the order parameter should follow the rule

$$\Delta T_{\max} \sim E^{2/3},$$

$$\chi_{\max} \sim E^{-1/3},$$

at the usually assumed linear temperature dependence of the coefficient α of the Landau expansion. For Rochelle salt sometimes the quadratic temperature dependence of α is used [16]:

$$\alpha = \alpha_0 \left[\left(T - \frac{T_{C1} + T_{C2}}{2} \right)^2 - \left(\frac{T_{C1} - T_{C2}}{2} \right)^2 \right],$$

(one can easily check that $\alpha(T_{C1}) = \alpha(T_{C2}) = 0$). It yields a different dependence for $\Delta T_{\max}(E)$

$$\Delta T_{\max} \approx 1 - \sqrt{1 + k'E^2/3},$$

with k' being the same for both lower and upper 'Curie points'. The obtained theoretical points for $|\Delta T_{\max}|$ and χ_{\max} , however, are poorly approximated by the above given dependences.

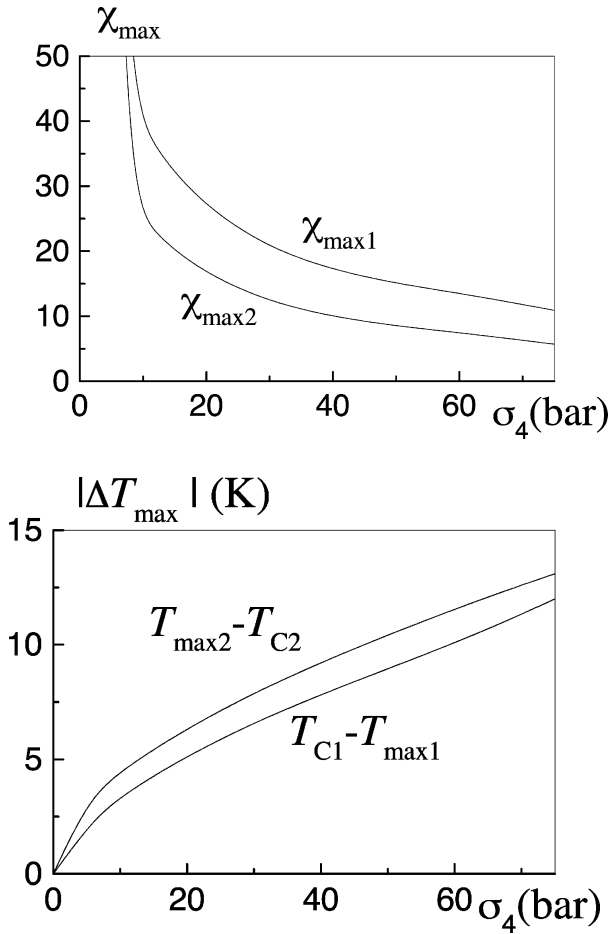


Fig. 3. Dependences of the maximal values of the free dielectric susceptibility χ_{11}^{σ} at the lower $\chi_{\max 1}$ and upper $\chi_{\max 2}$ transition points and their temperatures $|\Delta T_{\max}| = |T_{\max f} - T_{Cf}|$ on stress σ_4 .

In Fig. 4 we show the temperature curves of the elastic constant c_{44}^E at different stresses σ_4 . The stress smoothens the temperature dependences of c_{44}^E and increases with distance between its minima. The influence of stress is again seen in a temperature range from 235 K up to 255 K.

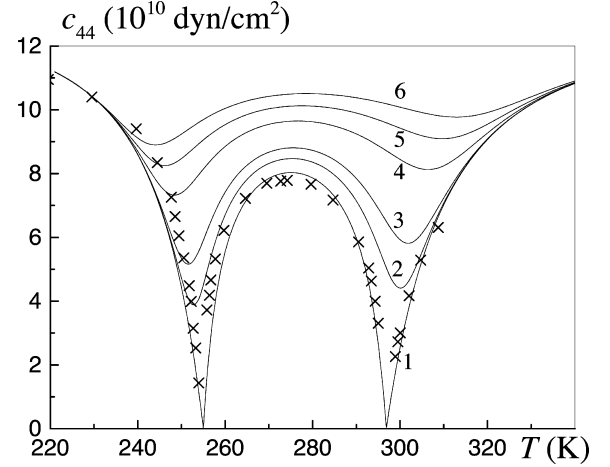


Fig. 4. Dependences of the elastic constant c_{44}^E on temperature at different stresses σ_4 . Notations and values of stress are the same as in Fig. 1. Experimental points are taken from [16].

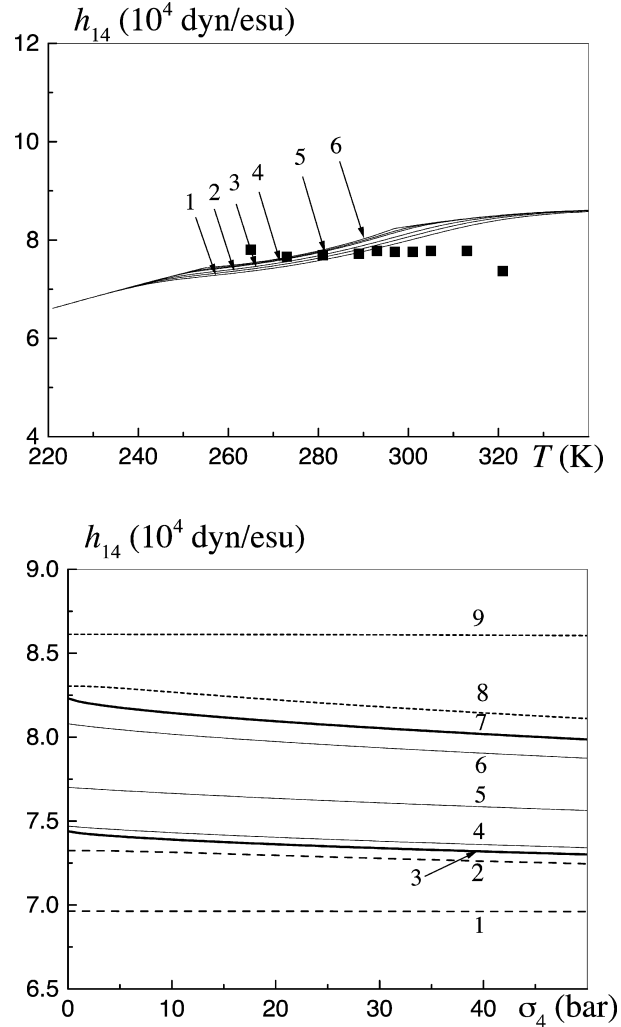


Fig. 5. Dependences of the piezomodule h_{14} on temperature at different stresses σ_4 and on stress σ_4 at different temperatures. Notations, values of temperature and stress are the same as in Fig. 1. Experimental points are taken from [17].

As one can see in Fig. 5, the shear stress σ_4 practically does not affect the constant of piezoelectric stress h_{14} at any temperature. Neither we have found any stress effects on the constant of piezoelectric strain g_{14} or the elastic constant at constant polarization c_{44}^E . At zero stress all these characteristics have only small bends at Curie points or no peculiarity at all.

In contrast to the presented above graphs, where the peak values of the characteristics were monotonously lowered down by the stress, dependence of the peak values of specific heat on this stress is non-monotonic. The maximal values of ΔC^σ at the ‘transition points’ are first strongly decreased, but at $\sigma_4 > 10$ bar they start to increase with σ_4 . Also, unlike in the figures below, these dependences are more pronounced at the lower ‘transition point’.

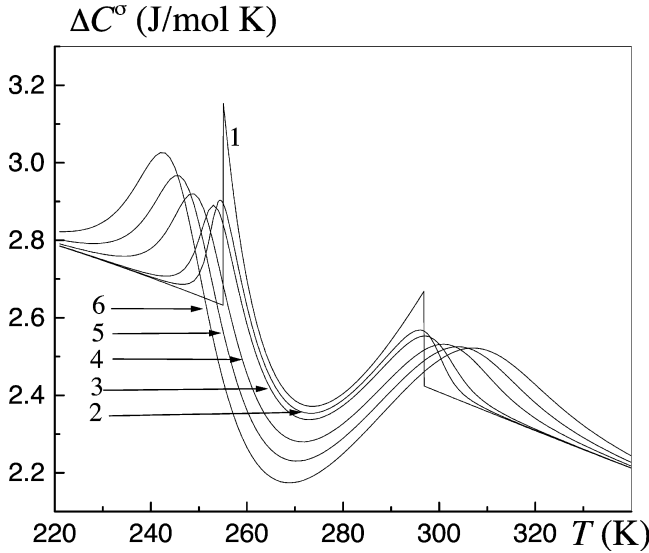


Fig. 6. Dependences of the specific heat C^σ on temperature at different stresses σ_4 . Notations and values of stress are the same as in Fig. 1.

Stress and temperature dependences of the relaxation time and imaginary parts of the dynamic dielectric permittivity are totally analogous to presented above dependences of static dielectric susceptibility and other characteristics having sharp peaks at the Curie points. More interesting are stress effects on the real part of the permittivity.

At frequencies below 5 GHz, the real part of the permittivity has a maximum at both Curie points. These maxima are lowered down and rounded off by the stress σ_4 (Fig. 7a) — similarly to those of a static dielectric susceptibility. At higher frequencies, the real part of the permittivity ϵ'_{11} has broad maxima around the Curie points and narrow minima within the broad peaks in the close vicinity of T_{Cf} . The higher frequency, the wider and deeper are the minima of ϵ'_{11} . Under the stress, the overall magnitude of the broad maxima is decreased, whereas the narrow minima are rounded off and raised up, until they vanish at all (Fig. 7b, c).

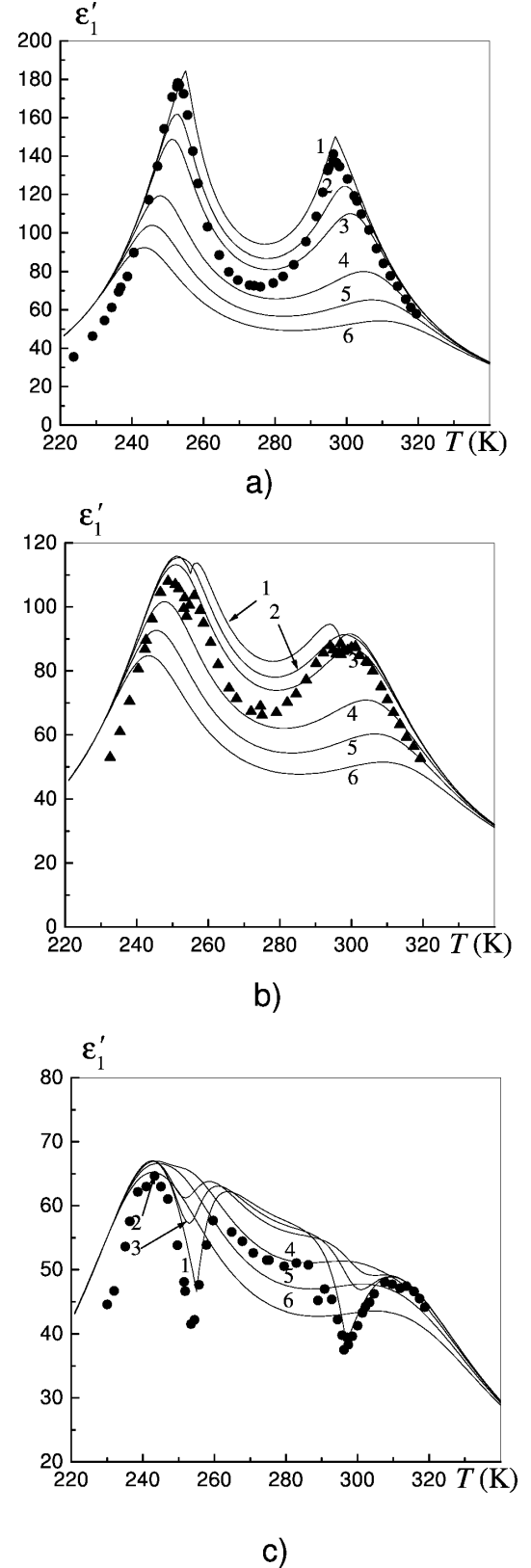


Fig. 7. Dependences of a real part of dynamic dielectric permittivity $\epsilon'_1(\nu)$ at $\nu = 3.0$ GHz (a), 5.1 GHz (b), and 9.45 GHz (c) on temperature at different stresses σ_4 and on stress σ_4 (right) at different temperatures. Notations and values of stress are the same as in Fig. 1. Experimental points are taken from [18].

IV. CONCLUSIONS

We presented a theoretical description of the stress σ_4 influence on the physical characteristics of Rochelle salt. Absent or very outdated experimental data for this influence, unfortunately, do not permit to verify the obtained results quantitatively.

The found dependences qualitatively accord with the available data and with the expected behaviour of the characteristics in external fields conjugate to the order parameter. The stress effects are visible in the ferroelectric phase and in some temperature range below T_{C1} and above T_{C2} . Since the stress σ_4 smears out the two second order phase transitions in Rochelle salt, overall its effects on the calculated quantities (second derivatives of the thermodynamic potential χ_{11}^σ , χ_{11}^ε , d_{14} , e_{14} , c_{44}^E and s_{44}^E , as well as ε_{11}'') are limited to smoothening of the peculiarities in their temperature curves (sharp maxima or minima at the Curie points). Stress effects on these quantities are more essential near the upper Curie point. The quantities that do not have large peculiarities at the transition points (c_{44}^P , h_{14} , g_{14}) are not affected by σ_4 . The stress influence on the pseudospin contribution to the specific heat is different. Dependence of the magnitude of the specific heat peaks at the 'transition points' is not monotonic and more pronounced near the lower 'Curie point'. At certain stress, the lower peak of the specific heat becomes even higher than at $\sigma_4 = 0$.

APPENDIX

The quantities $p_\xi^{\sigma_4}$ and $p_\sigma^{\sigma_4}$ entering the expression for specific heat (2.9) are

$$p_\xi^{\sigma_4} = \frac{\mu_1}{v} \left(\frac{\partial \xi}{\partial T} \right)_{\sigma_4} = p_\xi^{\varepsilon_4} + \varepsilon_\xi \alpha_4, \quad p_\sigma^{\sigma_4} = p_\sigma^{\varepsilon_4} + e_\sigma \alpha_4,$$

where

$$p_4 = \left(\frac{\partial \sigma_4}{\partial T} \right)_{p_1, \varepsilon_4} = \frac{1}{T} q_4^{p_1},$$

$$p_\xi^{\varepsilon_4} = \frac{\mu_1}{v} \frac{1}{\Delta_4} \left| \begin{array}{c} N_1^T N_{12} \\ N_2^T N_{22} \end{array} \right|, \quad \varepsilon_\xi = \frac{\mu_1}{v} \frac{1}{\Delta_4} \left| \begin{array}{c} N_1^{\varepsilon_4} N_{12} \\ N_2^{\varepsilon_4} N_{22} \end{array} \right|,$$

$$p_\sigma^{\varepsilon_4} = \frac{\mu_1}{v} \frac{1}{\Delta_4} \left| \begin{array}{c} N_{11} N_1^T \\ N_{21} N_2^T \end{array} \right|, \quad e_\sigma = \frac{\mu_1}{v} \frac{1}{\Delta_4} \left| \begin{array}{c} N_{11} N_1^{\varepsilon_4} \\ N_{21} N_2^{\varepsilon_4} \end{array} \right|,$$

$$N_1^T = -\frac{\gamma(1 - \xi^2 - \sigma^2) - 2\delta\xi\sigma}{2T},$$

$$N_2^T = \frac{\gamma(1 - \xi^2 - \sigma^2) - 2\gamma\xi\sigma}{2T};$$

$$N_{11} = \cosh \gamma + \cosh \delta - \frac{\beta}{2}(\tilde{J} + \tilde{K})\varkappa_4,$$

$$N_{12} = \frac{\beta}{2}(\tilde{J} - \tilde{K})\xi \sinh \delta,$$

$$N_{21} = \frac{\beta}{2}(\tilde{J} + \tilde{K})\sigma \sinh \gamma,$$

$$N_{22} = \cosh \gamma + \cosh \delta - \frac{\beta}{2}(\tilde{J} - \tilde{K})\varkappa_4,$$

$$N_1^{\varepsilon_4} = -2\beta\psi_4\varkappa_4,$$

$$N_2^{\varepsilon_4} = 2\beta\psi_4\sigma \sinh \gamma.$$

Notations used in the expression for dynamic dielectric permittivity are

$$K_0 = \left| \begin{array}{cc} a_{11} & a_{12} \\ a_{21} & a_{22} \end{array} \right|, \quad K_1 = a_{11} + a_{22},$$

$$K^{(0)} = -\left| \begin{array}{cc} a_{12} & a_1 \\ a_{22} & a_2 \end{array} \right|, \quad K^{(1)} = -a_1,$$

and

$$a_{11} = 1 - \frac{\tilde{J} + \tilde{K}}{T} \frac{1 - \cosh \gamma \cosh \delta}{(\cosh \gamma + \cosh \delta)^2},$$

$$a_{12} = \frac{\tilde{J} - \tilde{K}}{T} \frac{\sinh \gamma \sinh \delta}{(\cosh \gamma + \cosh \delta)^2},$$

$$a_{21} = \frac{\tilde{J} + \tilde{K}}{T} \frac{\sinh \gamma \sinh \delta}{(\cosh \gamma + \cosh \delta)^2},$$

$$a_{22} = 1 - \frac{\tilde{J} - \tilde{K}}{T} \frac{1 - \cosh \gamma \cosh \delta}{(\cosh \gamma + \cosh \delta)^2},$$

$$a_1 = \frac{4(1 - \cosh \gamma \cosh \delta)}{(\cosh \gamma + \cosh \delta)^2},$$

$$a_2 = \frac{4 \sinh \gamma \sinh \delta}{(\cosh \gamma + \cosh \delta)^2}.$$

- [1] T. Mitsui, Phys. Rev. **111**, 1259 (1958).
 [2] V. G. Vaks, *Vvedienie v mikroskopicheskuiu teoriiu signietoeliektrikov* (Nauka, Moscow, 1973), (in Russian).
 [3] B. Zeks, G. C. Shukla, R. Blinc, Phys. Rev. B. **3**, 2306 (1971).
 [4] B. Zeks, G. C. Shukla, R. Blinc, J. Phys. **33**, supplement to N 4, c2-67 (1972).

- [5] K. Mori, Ferroelectrics **31**, 173 (1981).
 [6] J. Kalenik, Acta Phys. Pol. A **48**, 387 (1975).
 [7] R. R. Levitskii, I. R. Zachek, V. I. Varanitskii, Ukr. Phys. J. **25**, 1766 (1980).
 [8] R. R. Levitskii, R. O. Sokolovskii, Condens. Matter Phys. **2**, 393 (1999).
 [9] R. R. Levitskii, I. R. Zachek, T. M. Verkholyak,

- A. P. Moina, Phys. Rev. B. **67**, 174112 (2003).
 [10] R. J. Glauber, J. Math. Phys. **4**, 294 (1963).
 [11] W. J. Bronowska, J. Appl. Crystallogr. **14**, 203 (1981).
 [12] R. D. Schulwass-Sorokina. Z. Phys. **73**, 700 (1932).
 [13] J. Hablützel, Helv. Phys. Acta **12**, 489 (1939).
 [14] W. Taylor, D. J. Lockwood, H. J. Labbe, J. Phys. C.: Solid State Phys. **17**, 3685 (1984).
 [15] I. V. Stasyuk, R. R. Levitskii, I. R. Zachek, A. P. Moina, Phys. Rev. B. **62**, 6198 (2000).
 [16] O. Yu. Serdobolskaya, Fiz. Tverd. Tela **38**, 1529 (1996).
 [17] W. P. Mason, Phys. Rev. **55**, 775 (1939).
 [18] F. Sandy, R. V. Jones, Phys. Rev. **168**, 481 (1968).

ВПЛИВ ЗСУВНОЇ НАПРУГИ σ_4 НА ФІЗИЧНІ ВЛАСТИВОСТІ СЕГНЕТОВОЇ СОЛИ

Р. Р. Левицький¹, І. Р. Зачек², А. П. Моїна¹, Т. М. Верхоляк¹

¹Інститут фізики конденсованих систем Національної академії наук України,
вул. Свенціцького, 1, Львів, 79011, Україна

²Національний університет "Львівська політехніка",
вул. С. Бандери, 12, Львів, 79013, Україна

Досліджено вплив зсувної напруги σ_4 на фазовий перехід, статичні й динамічні діелектричні, п'єзоелектричні, пружні й теплові властивості сегнетової соли. Дія цієї напруги помітна в сегнетоелектричній фазі та в деякій температурній ділянці — нижче від T_{C1} і вище від T_{C2} . Напруга розмиває два фазові переходи другого роду в кристалі, згладжує особливості температурних кривих других похідних термодинамічного потенціалу χ_{11}^σ , χ_{11}^ϵ , d_{14} , ϵ_{14} , c_{44}^E , s_{44}^E і ϵ_{11}^* . Дія напруги помітніша в околі верхньої точки Кюрі. Характеристики, які не мають особливостей у точках переходу (c_{44}^P , h_{14} , g_{14}), від напруги σ_4 практично не залежать. Барична залежність амплітуди піків теплоємності в "точках переходу" немонотонна й помітніша в околі нижньої "точки Кюрі".